

Identification of Immunodominant B-cell Epitope Regions of Reticulocyte Binding Proteins in *Plasmodium vivax* by Protein Microarray Based Immunoscreening

Jin-Hee Han¹, Jian Li^{1,2}, Bo Wang^{1,3}, Seong-Kyun Lee¹, Myat Htut Nyunt^{1,4}, Sunghun Na⁵, Jeong-Hyun Park⁶, Eun-Taek Han^{1,*}

¹Department of Medical Environmental Biology and Tropical Medicine, School of Medicine, Kangwon National University, Chuncheon 200-701, Korea; ²Department of Parasitology, College of Basic Medicine, Hubei University of Medicine, Shiyan, Hubei 442000, China; ³Department of Clinical Laboratory, The First Affiliated Hospital of Anhui Medical University, Hefei, Anhui, People's Republic of China; ⁴Department of Medical Research, Yangon, Myanmar; ⁵Department of Obstetrics and Gynecology and ⁶Department of Anatomy, School of Medicine, Kangwon National University, Chuncheon 200-701, Korea

Abstract: *Plasmodium falciparum* can invade all stages of red blood cells, while *Plasmodium vivax* can invade only reticulocytes. Although many *P. vivax* proteins have been discovered, their functions are largely unknown. Among them, *P. vivax* reticulocyte binding proteins (PvRBP1 and PvRBP2) recognize and bind to reticulocytes. Both proteins possess a C-terminal hydrophobic transmembrane domain, which drives adhesion to reticulocytes. PvRBP1 and PvRBP2 are large (> 326 kDa), which hinders identification of the functional domains. In this study, the complete genome information of the *P. vivax* RBP family was thoroughly analyzed using a prediction server with bioinformatics data to predict B-cell epitope domains. Eleven *pvrpb* family genes that included 2 pseudogenes and 9 full or partial length genes were selected and used to express recombinant proteins in a wheat germ cell-free system. The expressed proteins were used to evaluate the humoral immune response with vivax malaria patients and healthy individual serum samples by protein microarray. The recombinant fragments of 9 PvRBP proteins were successfully expressed; the soluble proteins ranged in molecular weight from 16 to 34 kDa. Evaluation of the humoral immune response to each recombinant PvRBP protein indicated a high antigenicity, with 38-88% sensitivity and 100% specificity. Of them, N-terminal parts of PvRBP2c (PVX_090325-1) and PvRBP2 like partial A (PVX_090330-1) elicited high antigenicity. In addition, the PvRBP2-like homologue B (PVX_116930) fragment was newly identified as high antigenicity and may be exploited as a potential antigenic candidate among the PvRBP family. The functional activity of the PvRBP family on merozoite invasion remains unknown.

Key words: *Plasmodium vivax*, reticulocyte binding protein, recombinant protein, antigenicity

INTRODUCTION

An estimated 124-283 million of malaria clinical cases occur annually, and the disease continues to be a serious health threat in developing countries [1]. Malaria is caused by *Plasmodium* spp., and of them *Plasmodium vivax* is geographically the most widely spread species [2]. Moreover, control and understanding of vivax malaria have limitation from lack of *P. vivax* continuous culture [3-5]. To overcome this constraint, various new approaches using bioinformatics data were tried and used

for development of antimalarial drugs and vaccines [6,7].

In the blood stage, *Plasmodium* spp. invade erythrocytes or reticulocytes by use of an actin-myosin motor [8,9]. This process internalizes the parasite in red blood cells (RBCs), followed by growth and replication to form the merozoites. The invasive merozoites egress from infected RBCs to invade new host cells [10-12]. In this step, specific receptors on the surface of host RBCs are required for interaction involved with attachment, reorientation, and junction formation for parasite invasion [12]. During these multiple steps, many proteins mediate the interaction between RBCs and parasites [13,14]. One of these proteins is Duffy binding protein of *P. vivax* (PvDBP), which is essential for invasion of vivax parasites into RBCs. The invasion utilizes the Duffy antigen/receptor for chemokines (DARC) on the surface of RBCs [15,16]. PvDBP and DARC were only one of the unique and essential ligand-recep-

•Received 28 February 2015, revised 23 July 2015, accepted 23 July 2015.

*Corresponding author (ethan@kangwon.ac.kr)

© 2015, Korean Society for Parasitology and Tropical Medicine

This is an Open Access article distributed under the terms of the Creative Commons Attribution Non-Commercial License (<http://creativecommons.org/licenses/by-nc/3.0>) which permits unrestricted non-commercial use, distribution, and reproduction in any medium, provided the original work is properly cited.

tors for erythrocyte invasion of *P. vivax* [17]. Recently, clinical vivax patients were observed in Duffy-negative populations of Madagascar, where mixture of Duffy-positive and Duffy-negative populations has lived together [18]. Thus, new questions have arisen with regards to the Duffy-independent *P. vivax* invasion of erythrocytes.

Reticulocyte binding-like (RBL) family proteins are possible candidates for alternative invasion pathway after PvDBP-DARC interaction. RBL proteins may interact with reticulocytes by an independent pathway with the Duffy phenotype, suggesting that the RBL family may use a novel receptor for reticulocyte invasion. RBL proteins feature a small and large exon separated by a small intron, and the small exon encodes the signal peptide [19,20]. The complete gene sequence of *P. vivax* Salvador I (Sal-1) strain comprises genes for 11 *P. vivax* reticulocyte binding proteins (PvRBP) as well as 2 pseudogenes [14,21]. Five of these genes are highly expressed in schizont stage during the erythrocytic stage of *P. vivax* parasites [22,23]. However, no studies have addressed the antigenicity of PvRBPs from vivax malaria patients in endemic countries.

In infectious diseases, identification of the antigenic domain(s) is important for diagnosis and vaccine development [24,25]. Numerous studies supported the accuracy of the specific domain prediction such as B-cell epitopes in infectious diseases [24-26]. Several B-cell epitope prediction systems based on bioinformatics data including ABCpred, BcePred, and BepiPred have been reported [27-33]. ABCpred predicts B-cell epitopes in an antigen sequence using an artificial recurrent neural network. This program is able to predict epitopes with 65.9% accuracy [29,31]. BcePred predicts linear B-cell epitopes on the basis of their physico-chemical properties (hydrophilicity, flexibility, mobility, acces-

sibility, polarity, exposed surface, and turns) and produces epitopes with 58.7% accuracy using flexibility, hydrophilicity, polarity, and exposed surface factor score combined at a recommendation threshold of 2.38 [28]. The BepiPred server has been used to predict the location of linear B-cell epitopes using a combination of a hidden Markov model and propensity scale method [30,34]. This B-cell epitope prediction might be useful to decide antigenic domains in the *P. vivax* RBL family proteins. This information would be helpful for increased understanding of the PvRBP family as a potential antigenic candidate.

In the present study, PvRBP family protein sequences were analyzed to predict B-cell epitope domains by in-silico data mining. Each recombinant PvRBP including B-cell epitope domains was expressed in a wheat germ cell-free expression system (WGCF). The humoral immune responses against PvRBPs were observed to evaluate the probability of a potential antigenic candidate by protein microarray-based serological screening.

MATERIALS AND METHODS

Human serum and parasite samples

Human serum samples were collected from 16 *P. vivax* positive patients from an endemic area of Gangwon-do (Province), Republic of Korea (Korea). Vivax infections were confirmed by microscopic examination and detection of malaria antigen by P.f/Pan rapid diagnosis test kit (SDFK60) (SD Diagnostics, Giheung, Korea). Serum samples were collected from 8 healthy individuals with no history of malaria living in non-endemic areas of Gangwon-do. This study was approved by the Institutional Review Board at Kangwon National University Hospital.

Table 1. General information of *Plasmodium vivax* reticulocyte binding like protein (PvRBP)

Name	Gene ID (PVX_)	Chromosome No.	Length (aa)	MW (kDa)	SP	TM	Expression stage	Note	Reference
PvRBP1a	098585	7	2,833	326.2	Y	Y	Schizont	Full length	[19,23]
PvRBP1b	098582	7	2,608	303.3	Y	N	Unknown	Full length	[14]
PvRBP1 like-partial	125738	NA	785	90.9	N	Y	Unknown	Partial length	[14]
PvRBP2a	121920	14	2,487	286.6	Y	N	Schizont	Full length	[14,21]
PvRBP2b	094255	8	2,806	325.5	Y	N	Schizont	Full length	[14,21]
PvRBP2c	090325	5	2,824	326.4	Y	Y	Schizont	Full length	[19,23]
PvRBP2 like-partial A	090330	5	623	72.8	Y	N	Schizont	Partial length	[14,21]
PvRBP2 like-partial B	101590	14	640	74.2	Y	N	Unknown	Partial length	[14,21]
PvRBP2 like-homologue B	116930	12	1,060	123.9	Y	N	Unknown	Full length	[14,21]
PvRBP2d	101585	14	2,829	329.1	Y	Y	Null	Pseudogene	[21]
PvRBP3	101495	14	2,798	323.1	N	Y	Null	Pseudogene	[21]

aa, amino acid; MW, molecular weight; kDa, kilodalton; SP, signal peptide; TM, transmembrane domain; NA, not assigned.

The individual serum samples were examined for humoral immune responses by protein array. Genomic DNA was extracted from 200 µl whole blood of the *P. vivax* patients using QIAamp DNA Blood Mini Kits (Qiagen, Hilden, Germany) according to the manufacturer's protocol.

Prediction of linear B-cell epitopes for PvRBP family

The in-silico prediction of linear B-cell epitopes was conducted by ABCpred (<http://imtech.res.in/raghava/abcpred/>), BcePred (<http://www.imtech.res.in/raghava/bcepred/>), and BepiPred (<http://www.cbs.dtu.dk/services/BepiPred/>) to heighten the accuracy. For prediction of B-cell epitopes, PvRBP family sequences were obtained from PlasmoDB (<http://plasmodb.org/plasmo/>) (Table 1). Each sequence was allowed in the B-cell epitope prediction with each prediction server. ABCpred setting was up to 20 mer peptides by overlapping filter and a threshold value of 0.51 (ABCpred base threshold value). The predicted B-cell epitopes were ranked according to their score obtained by a trained recurrent neural network. Higher scores (>0.90) were chosen for B-cell epitope combination analysis for each protein. BcePred predicted linear B-cell epitopes based on physico-chemical properties using values of hydrophilicity (2.0), flexibility (1.9), accessibility (2.0), turns

(1.9), exposed surface value (2.4), polarity (2.3), and antigenic propensity (1.8) to calculate a threshold value at 1.9. BepiPred 1.0 was set for each PvRBPs sequence using a threshold value of 1.3, which represented B-cell epitope prediction sensitivity and specificity of 13% and 96%, respectively. Each PvRBP family was analyzed for flexibility, antigenic index, and surface location by the Protean protein secondary structure prediction program (Lasergene, Madison, Wisconsin, USA). Finally, 20 PvRBP family fragments were selected from the combination of predicted B-cell epitopes listed from the highest scores for humoral immune response analysis.

Expression of recombinant PvRBPs B-cell epitope fragments

PvRBP family sequences from PlasmoDB were used to design primers of gene amplification for B-cell epitope fragments (Table 2). Expected molecular weight and isoelectric point for B-cell epitope fragments are shown in Table 2. For recombinant protein expression vector construction, pEU-E01-His-TEV-MCS vector containing a 6× His tag at the N-terminus (CellFree Science, Matsuyama, Japan) was used. After restriction enzyme digestion of pEU vector with *XhoI* and *BamHI*, the target amplicon was cloned into the pEU vector by an In-

Table 2. Primer sequences for recombinant PvRBP family protein expressions

Fragment (PVX ₁)	Forward primer (5'→3')	Reverse primer (5'→3')	Position (aa)	Length (aa)	pI	MW (kDa)
098585-1	CAAAACAGCATGCAGCAGTAC	TTCGTCTACTTCCCCTTTTGATGT	804-1,073	270	5.1	34.4
098585-2	GAAATGAATCTAAAAAGAGCGCT	TTCTTCTTTGTTTTCTGGGTTCA	2,619-2,822	204	4.2	25.6
098582-1	GTAGATTTAAATCGAGGGAAAAACAC	GCAGCTGGATTGCTTCAAA	15-289	273	6.7	34.7
098582-2	GATAAGTTGAAAGCAGAACTAGGAAGT	GATCTGTTGTGTTTCTCTTCC	996-1,254	259	5.6	33.8
125738-1	CTAGAAAATGACAAAAGGAAAAAGAGC	AATGTCTGTTTGAGGGGGTAGTC	476-623	148	4.6	20.0
125738-2	AAAAATGACAGAAACGATCAAAAAT	ATCTTTTACATTACGTTTTGAACCATT	630-772	143	5.4	18.9
121920-1	TCAAGCAAAGAAAGCAATCG	TATTTGATTCTTTGGTGTGAAGAGAA	20-145	126	9.7	17.7
121920-2	AGCGAAAAATAGATAAAAATTTGGA	CATATCGTCGACTAATCTTTTAAGTC	453-713	261	5.2	33.3
121920-3	ACGGAAGCTAAAACACTCAGG	TGTGTGTAATCTTATCATCCGT	1,789-2,049	261	5.8	32.9
121920-4	GCTAAGGAAAACCTCCATTAATATGC	TTCTTCCCTTCTTGAAGATTTCCA	2,330-2,474	145	7.4	19.0
094255-1	CAAGAAGCTTCCCTACCAAAATGC	TGCAATATTCACTTTCTTAATGGAGT	728-965	238	4.7	30.7
094255-2	GATACCCAAGAGAACGATACAGAC	TTCAGAATAATCGCTATTGTGCGAA	2,673-2,806	134	4	18.2
090325-1	AGGAATGGTCAACACAAATACAAC	TACAATTCAGGGGCCTCTG	47-171	125	9.7	18.0
090325-2	CTAAAAGCAAGCTCGAACGATC	GTATTTATCAGCATTTGATTTCAATTC	2,115-2,314	200	5	25.7
090325-3	GCAAAAGTTGAGCCTGAAGC	ATCTTCTTCATTAAGCAAACCTCG	2,652-2,824	173	3.9	22.3
090330-1	AGGGATGATCAAAACGGACA	TGAATTTGGAACACTATGCAATTC	47-145	99	8.4	14.4
090330-2	GAAAATCCAGAACACTATAAAAATAAGAGA	AATTTTCATCTATTACGAAATCTGCC	242-370	129	6.8	18.5
101590-1	AAGGATGTCAATCGAAACAAACC	ATGCAATTTTTTATTATCATCTTCCAT	22-145	124	7.5	17.2
116930-1	TTGCACAATTCGACCTCC	AACCATGCTGCCTTCGTAC	359-477	119	6.3	16.6
116930-2	GATAACATCAAGAGGAGGAACGC	CAGTTTGAAATTTTTATCGATGTTGT	603-736	134	9.7	19.4

pI, isoelectric point.

fusion cloning system (Clontech, Mountain View, California, USA). The sequences of each protein fragment were analyzed using an ABI 3700 genetic analyzer (Genotech, Daejeon, Korea) and were used for small-scale WGC expression in the Cell-Free Expression Kit (CellFree Sciences) according to the manufacturer's protocol. Recombinant crude protein (10 µl) was mixed with reducing sample buffer and total and soluble fractions were obtained by centrifugation (12,000 g). For target protein detection, recombinant proteins were separated using 12% SDS-PAGE and detected by Western blot analysis. Briefly, the electrophoretically resolved proteins were transferred to polyvinyl difluoride membranes (Millipore, Bedford, Massachusetts, USA). Specific proteins were detected by mouse anti-penta-His antibody (Qiagen) in a 1:2,000 dilution of 0.2% Tween 20 in phosphate-buffered saline (PBS-T). The primary antibody reaction was detected by a 1:5,000 dilution of goat anti-mouse IRDye CW800 secondary antibody (LI-COR Biosciences, Lincoln, Nebraska, USA) in PBS-T. Western blot results were determined with an Odyssey infrared imaging system and incorporated software (LI-COR Biosciences) at a wavelength of 680 nm.

Analysis of humoral immune responses to recombinant PvRBPs

For humoral immune response analysis, the protein array analysis was done as follows. Tri-amine coated slides were prepared by trimethoxysilane (Sigma-Aldrich, St Louis, Missouri, USA) on the microscope slide (Marienfeld-Superior, Lauda, Germany). The crude recombinant protein fragment (1 µl) of PvRBP was reacted to the amine-coated slide surface. After washing and blocking with PBS-T containing 5% bovine serum albumin (BSA), the array was probed with serial dilution (1:100 to 1:10) of malaria patient or healthy individual sera and with a 1:100 dilution of wheat germ lysate in PBS. Array conditions were optimized using 1:10 dilution of mixed sera from patients and healthy individuals. Alexa Fluor 546 goat anti-human IgG (Invitrogen) in PBS-T containing 1% BSA was applied into each spots for detection of the antibody reaction. The fluorescent signals were detected using a ScanArray Express fluorescence scanner (PerkinElmer, Boston, Massachusetts, USA). The cut-off value was defined as 3 standard deviations (SDs) above the mean fluorescence intensity (MFI) of the healthy individual samples. Recombinant *P. vivax* merozoite surface protein 1-19 (PvMSP1-19) was used as a positive control, and its MFIs were used for compensation in each slide.

Statistical analysis

Data were analyzed using GraphPad Prism (GraphPad Software, San Diego, California, USA) and Excel 2013 (Microsoft, Redmond, Washington, USA). Statistical analysis of significance between *P. vivax* parasite-infected patients and healthy individual samples was performed with 2-tailed non-parametric Mann-Whitney U test. A *P*-value of <0.05 was considered statistically significant.

RESULTS

Bioinformatics analysis of *pvr*bp gene sequences

A total of 11 *pvr*bps genes including 3 homologue gene sub-families of the PvRBP family (*pvr*bp1s, *pvr*bp2s, and *pvr*bp3) (Table 1) were selected for this study. The 3 *pvr*bp1 homologue genes in *P. vivax* Sal-1 included *pvr*bp1a (PVX_098585), *pvr*bp1b (PVX_098582), and *pvr*bp1-like partial sequence (PVX_125738) (Fig. 1). *Pvr*bp1a and *pvr*bp1b encoded signal sequence at the N-terminal region in a full-length sequence. *Pvr*bp1a and *pvr*bp1-like partial sequence displayed a transmembrane domain near the C-terminus (Table 2). This *pvr*bp1-like partial sequence had 95% similarity with the C-terminal sequence of *pvr*bp1b, and was consistent with the typical RBL family structure.

The *pvr*bp2 genes comprise 7 members that include *pvr*bp2a (PVX_121920), *pvr*bp2b (PVX_094255), *pvr*bp2c (PVX_121920), *pvr*bp2d (PVX_101585), *pvr*bp2 like partial A (PVX_090330), *pvr*bp2 like partial B (PVX_101590), and *pvr*bp2 homologue B (PVX_116930) (Fig. 1). *Pvr*bp2d was identified as a pseudogene. The other 6 *pvr*bp2 homologue genes comprise 4 members with a full length sequence and 2 members with a partial sequence (Table 1). Among the *pvr*bp2 genes, signal sequence and transmembrane domain were identified in *pvr*bp2c. Unlike other *pvr*bp genes, the *pvr*bp2 homologue B gene consists of introns at both N-terminus and C-terminus, and displayed a shorter open reading frame (1,060 aa, 123.9 kDa) than those of other *pvr*bp sequences. Cysteine (Cys) residues and alpha helix coiled-coil region ectodomain structure were detected in *pvr*bp2 homologue B. Accordingly, the *pvr*bp2 homologue B was expected to evoke a higher immune response. *Pvr*bp3 (PVX_101495) was observed as a pseudogene in the Sal-1 strain. All members of the *pvr*bps displayed large molecular weights exceeding 280 kDa and similar protein structure consisting of many Cys residues (Table 1; Fig. 1).

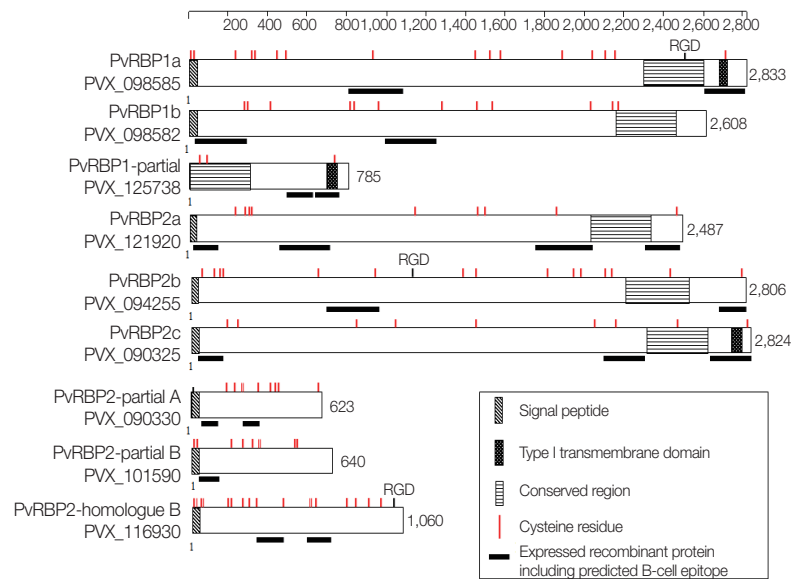


Fig. 1. Schematic protein features and secondary structures of the PvRBP family. The PvRBP family based on amino acid (aa) length. Black bar denotes fragment for recombinant protein expression, with the order of fragment number from the N-terminal region. RGD, arginyl-glycyl-aspartic acid a cell adhesion motif.

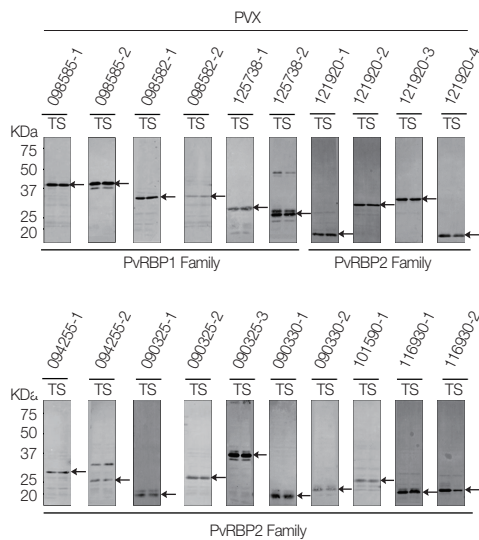


Fig. 2. Recombinant protein expressions of PvRBP family fragments by Western blot analysis. All the PvRBP recombinant proteins were expressed in the supernatant as the soluble fraction with variable expression level in the wheat germ cell-free expression system. The expression level of each PvRBP protein was detected by Western blot analysis probed with anti-His tag. kDa, kilodalton; T, total crude protein; S, supernatant soluble fraction.

Prediction of B-cell epitopes for PvRBPs

The prediction results of B-cell epitopes obtained by the 3 different B-cell prediction servers and protein fragment information are shown in Table 2. The prediction results of linear B-cell epitopes for PvRBP family displayed a wide range of fragments (3 to 29; median 13.9). According to the protein secondary structures and high probability of surface exposure, 20 fragments were selected as the potential specific B-cell epitopes for further study. The prediction results revealed that 5 fragments were located in the N-terminal region (PVX_098582-1, PVX_121920-1, PVX_090325-1, PVX_090330-1, and PVX_101590-1) and another 5 at the C-terminus (PVX_098585-2, PVX_125738-2, PVX_121920-4, PVX_094255-2, and PVX_090325-3). The specific domain feature contained alpha helix coiled-coil domain in 4 PvRBPs (PVX_098582-2, PVX_125738-1, PVX_090325-2, and PVX_090330-2) and repeat sequence with low complexity in 5 PvRBPs (PVX_098585-1, PVX_121920-2, PVX_121920-3, PVX_094255-1, and PVX_116930-2). PvRBP2-like homologue B fragment 1 (PVX_116930-1) did not represent any specific feature on protein secondary structure prediction. According to the B-cell epitope prediction, all of the fragments were likely to be surface-exposed and expected to be potentially antigenic.

opes for PvRBP family displayed a wide range of fragments (3 to 29; median 13.9). According to the protein secondary structures and high probability of surface exposure, 20 fragments were selected as the potential specific B-cell epitopes for further study. The prediction results revealed that 5 fragments were located in the N-terminal region (PVX_098582-1, PVX_121920-1, PVX_090325-1, PVX_090330-1, and PVX_101590-1) and another 5 at the C-terminus (PVX_098585-2, PVX_125738-2, PVX_121920-4, PVX_094255-2, and PVX_090325-3). The specific domain feature contained alpha helix coiled-coil domain in 4 PvRBPs (PVX_098582-2, PVX_125738-1, PVX_090325-2, and PVX_090330-2) and repeat sequence with low complexity in 5 PvRBPs (PVX_098585-1, PVX_121920-2, PVX_121920-3, PVX_094255-1, and PVX_116930-2). PvRBP2-like homologue B fragment 1 (PVX_116930-1) did not represent any specific feature on protein secondary structure prediction. According to the B-cell epitope prediction, all of the fragments were likely to be surface-exposed and expected to be potentially antigenic.

Expression of recombinant PvRBP protein fragments by cell-free expression system

All the PvRBP recombinant proteins were expressed in the supernatant as the soluble fraction with variable expression level in the WGC system. The expression level of the specific PvRBP proteins was confirmed by Western blot analysis with

Table 3. Total IgG prevalence of each recombinant PvRBP protein including predicted B-cell epitope domain

Antigen (PVX_)	No. of patients samples (n)			95% CI ^b (%)	MFI ^c	No. of healthy samples (n)			95% CI (%)	MFI	P-value ^e	Features/ Structures
	Posit.	Neg.	Total (%) ^a			Posit.	Neg.	Total (%) ^d				
098585-1	10	6	16 (62.5)	38.6-81.5	6,429	0	8	8 (100.0)	67.6-100.0	3,139	0.0013	Repeat sequence
098585-2	8	8	16 (50.0)	28.0-72.0	5,480	0	8	8 (100.0)	67.6-100.0	2,943	0.0016	C-terminal
098582-1	6	10	16 (37.5)	18.5-61.4	5,806	0	8	8 (100.0)	67.6-100.0	3,275	0.0011	N-terminal
098582-2	10	6	16 (62.5)	38.6-81.5	6,566	0	8	8 (100.0)	67.6-100.0	3,181	0.0004	Coiled coil
125738-1	11	5	16 (68.8)	44.4-85.8	9,242	0	8	8 (100.0)	67.6-100.0	3,970	0.0002	Coiled coil
125738-2	11	5	16 (68.8)	44.4-85.8	10,280	0	8	8 (100.0)	67.6-100.0	3,741	0.0003	C-terminal
121920-1	11	5	16 (68.8)	44.4-85.8	11,283	0	8	8 (100.0)	67.6-100.0	4,628	0.0013	N-terminal
121920-2	11	5	16 (68.8)	44.4-85.8	9,232	0	8	8 (100.0)	67.6-100.0	3,863	0.0007	Low complexity
121920-3	11	5	16 (68.8)	44.4-85.8	8,821	0	8	8 (100.0)	67.6-100.0	3,010	0.0005	Repeat sequence
121920-4	6	10	16 (37.5)	18.5-61.4	6,947	0	8	8 (100.0)	67.6-100.0	3,710	0.0053	C-terminal
094255-1	12	4	16 (75.0)	50.5-89.8	13,325	0	8	8 (100.0)	67.6-100.0	5,163	0.0007	Repeat sequence
094255-2	8	8	16 (62.5)	28.0-72.0	6,307	0	8	8 (100.0)	67.6-100.0	3,394	0.0011	C-terminal
090325-1	14	2	16 (87.5)	64.0-96.5	17,597	0	8	8 (100.0)	67.6-100.0	6,257	0.0002	N-terminal
090325-2	9	7	16 (56.3)	33.2-76.9	19,179	0	8	8 (100.0)	67.6-100.0	7,226	0.0004	Short coiled coil
090325-3	11	5	16 (68.8)	44.4-85.8	18,615	0	8	8 (100.0)	67.6-100.0	6,095	0.0007	C-terminal
090330-1	13	3	16 (81.3)	57.0-93.0	12,413	0	8	8 (100.0)	67.6-100.0	4,455	0.0002	N-terminal
090330-2	7	9	16 (43.8)	23.1-66.8	12,149	0	8	8 (100.0)	67.6-100.0	6,072	0.0030	Short coiled coil
101590-1	9	7	16 (56.3)	33.1-76.9	7,223	0	8	8 (100.0)	67.6-100.0	3,299	0.0005	N-terminal
116930-1	12	4	16 (75.0)	50.5-89.8	12,407	0	8	8 (100.0)	67.6-100.0	4,522	0.0004	Short coiled coil
116930-2	14	2	16 (87.5)	64.0-96.5	11,332	0	8	8 (100.0)	67.6-100.0	3,346	0.0005	Repeat sequence
PvMSP1-19	4	0	4 (100.0)	51.0-100.0	9,987	0	8	8 (100.0)	67.6-100.0	1,887	0.0286	

^aSensitivity, percentage of positives in patient samples.

^bCI, confidence intervals.

^cMFI, mean fluorescence intensity.

^dSpecificity, percentage of negatives in healthy samples.

^eDifferences in the total IgG prevalence for each antigen between patients and healthy individuals were calculated with Mann-Whitney U test. $P < 0.05$ considered as statistically significant.

anti-His tag for detection of recombinant protein (Fig. 2). Lower pI values of expressed PvRBP proteins were slower-migrating proteins on the SDS-PAGE analysis. The experimental positive control was PvMSP1-19, which was expressed by WGCF and purified by Ni-affinity chromatography as described previously [35]. These recombinant proteins were used for further analysis.

Humoral immune responses analysis of recombinant PvRBP proteins by protein microarray

The humoral immune responses of the PvRBP family fragment proteins were evaluated with sera from *P. vivax* patients and healthy individuals by protein microarray (Table 3). IgG prevalence to recombinant PVX_090325-1 and PVX_116930-2 fragments had the highest sensitivity (87.5%). Similarly, recombinant PvRBP2 fragments displayed high IgG positive responses; PVX_090330-1 (81.3%), PVX_094255-1 (75.0%), and PVX_116930-1 (75.0%) (Table 3). Recombinant PvRBP proteins from 6 fragments involving 2 fragments of PVX_125738

(coiled-coil and putative C-terminal domains), PVX_121920-1, -2, and -3 (N-terminal fragment, low complexity sequence, and repeat sequence, respectively), and PVX_090325-3 (C-terminal fragment) showed a similarly of 68.8% IgG-positive responses. Other fragments including PVX_098585-1 (repeat sequence), PVX_098582-2 (coiled-coil domain), and PVX_094255-2 (C-terminal domain) were 62.5% IgG-positive responses. The IgG prevalence below 60.0% was detected in PVX_090325-2 (containing a short coiled-coil domain), PVX_101590-1 (N-terminal region), PVX_098585-2 (C-terminal region), PVX_090330-2 (contained short coiled-coil domain), PVX_098582-1 (N-terminal region), and PVX_121920-4 (C-terminal region) (Table 3). The IgG prevalence of the overall PvRBP2s was higher than those of PvRBP1s. Recombinant PvRBP2 fragments displayed high positivity of IgG at the N-termini and repeat sequence regions. Most of recombinant PvRBP fragments showed high specificities and significantly different between *P. vivax* patients and healthy individuals ($P < 0.05$; Table 3).

DISCUSSION

In the post-genomic era, the *P. vivax* complete genome sequences and bioinformatics information are available for various proteome-related approaches [14,34,36-38]. Bioinformatics tools for selection of proteins in *P. falciparum* have been used for new malaria antigenic protein identification. Antigenic proteins were considered from secondary structures, such as the alpha helical coiled-coil domain [36,39]. In this study, humoral immune responses against recombinant PvRBP family proteins were evaluated by integration of bioinformatics with 3 prediction servers for B-cell epitopes, cell-free protein expression system, and protein microarray methods. The advantage of this strategy is easy selection of possible antigenic proteins and the ability to evaluate antigenicity in a small quantity of recombinant proteins.

A higher humoral immune response level was observed in PVX_116930-1 (391-510 aa) and PVX_116930-2 (635-769 aa) than those of the other PvRBP family genes (75.0% and 87.5%, respectively) (Table 3). Especially, PVX_116930-2 contained the sequence (₆₆₃KSPEPL₆₉₂) that was repeated 5 times, possibly to elicit high antigenicity. Although this protein expression level was not specific in schizont stage, overall it was highly conserved regardless of the strain [40]. BLAST analysis revealed a close relationship with *P. falciparum* conserved protein (PF3D7_0305200) and PvRBP2 homologue B (PVX_116930) with a 41% sequence similarity in alpha helical coiled-coil domains. Although the exact function of the PF3D7_0305200 has not yet been defined, it has the expected high antigenicity [13,41-43]. This evidence supports the potential of PvRBP2 homologue B (PVX_116930) as an antigenic serological marker. The alpha helical coiled-coil domain has demonstrated high antigenicity in a broad variety of antigens of parasites that include *Plasmodium* spp. [38,39,43]. The recombinant proteins as coiled-coil domain elicit the antigenicity, consistent with previous studies [36,38,39,44]. PvRBP2 homologue B may an important antigenic protein of the PvRBP family and could be useful serological markers for *P. vivax*.

Although the similarity of PvRBP family gene sequence was low, these homologue genes presented a typical RBL family structure, which consisted of a large exon (ectodomain) and small cytoplasmic tails, such as type 1 transmembrane proteins. The PvRBP family has an expected specific function involved in reticulocyte recognition during host cell invasion [19]. The typical RBL family proteins, PvRBP1a and PvRBP2c, bind to reticulocytes [19,20]. Transcription results of the

PvRBP family indicate that RBP1a is highly expressed during blood stage parasites. Presently, a new antigenic RBP protein, PvRBP2 homologue B, was confirmed to be consistently expressed during blood stage parasite development. Localization, expression level and pattern, and reticulocyte binding ability of this protein need to be explored.

The sequence diversity analysis of PvRBP1 revealed that the N-terminal region of the protein contains polymorphic residues with non-synonymous polymorphisms relating with immune selection pressure [44,45]. In contrast, PvRBP2 homologue B is highly conserved in worldwide isolate; however, coiled-coil domain has immune selection. In this study, antigenicity of most of the PvRBP2 family including the PvRBP2 homologue B was higher than that of the PvRBP1 family. This result may reflect the high genetic diversity in PvRBP2 compared to PvRBP1 [46]. Moreover, high prevalence of total IgG represents the repeat sequence and both termini of PvRBP2 family. Especially N-terminal part of PvRBP2c (PVX_090325-1) and PvRBP2 partial A (PVX_090330-1) represent high antigenicity (87.5% and 81.3%, respectively) with sequence similarity (60%). These domains may also play an important role for recognition of antibodies.

In summary, this study is the first evaluation of the humoral immune responses against fragments of PvRBP family proteins with predicted B-cell epitope regions in vivax malaria patients and healthy individuals. A high prevalence of total IgG against the fragment of PvRBP2 homologue B (PVX_116930) was detected, implicating the fragment as a potential serological marker. A high prevalence of total IgG in PvRBP2 family genes was observed in the alpha helical coiled-coil motif and at the N-terminus. The present findings will be valuable for serological marker candidates.

ACKNOWLEDGMENT

This work was supported by a grant from the Korea Health Technology R&D Project, Ministry of Health & Welfare, Republic of Korea (A121180).

REFERENCES

1. World Health Organization. World Malaria Report (2014). 2014.
2. Gething PW, Elyazar IR, Moyes CL, Smith DL, Battle KE, Guerra CA, Patil AP, Tatem AJ, Howes RE, Myers ME, George DB, Horby P, Wertheim HF, Price RN, Mueller I, Baird JK, Hay SI. A long ne-

- glected world malaria map: *Plasmodium vivax* endemicity in 2010. *PLoS Negl Trop Dis* 2012; 6: e1814.
3. Birkett AJ, Moorthy VS, Loucq C, Chitnis CE, Kaslow DC. Malaria vaccine R&D in the Decade of Vaccines: breakthroughs, challenges and opportunities. *Vaccine* 2013; 31 (suppl 2): B233-B243.
 4. Noulin F, Borlon C, Van Den Abbeele J, D'Alessandro U, Erhart A. 1912-2012: a century of research on *Plasmodium vivax* in vitro culture. *Trends Parasitol* 2013; 29: 286-294.
 5. Udomsangpetch R, Kaneko O, Chotivanich K, Sattabongkot J. Cultivation of *Plasmodium vivax*. *Trends Parasitol* 2008; 24: 85-88.
 6. Ubaida Mohien C, Colquhoun DR, Mathias DK, Gibbons JG, Armistead JS, Rodriguez MC, Rodriguez MH, Edwards NJ, Hartler J, Thallinger GG, Graham DR, Martinez-Barnette J, Rokas A, Dinglasan RR. A bioinformatics approach for integrated transcriptomic and proteomic comparative analyses of model and non-sequenced anopheline vectors of human malaria parasites. *Mol Cell Proteomics* 2013; 12: 120-131.
 7. Fard AT, Salman A, Kazemi B, Bokhari H. In silico comparative genome analysis of malaria parasite *Plasmodium falciparum* and *Plasmodium vivax* chromosome 4. *Parasitol Res* 2009; 104: 1361-1364.
 8. Jones ML, Kitson EL, Rayner JC. *Plasmodium falciparum* erythrocyte invasion: a conserved myosin associated complex. *Mol Biochem Parasitol* 2006; 147: 74-84.
 9. Keeley A, Soldati D. The glideosome: a molecular machine powering motility and host-cell invasion by Apicomplexa. *Trends Cell Biol* 2004; 14: 528-532.
 10. Cowman AE, Crabb BS. Invasion of red blood cells by malaria parasites. *Cell* 2006; 124: 755-766.
 11. Wright GJ, Rayner JC. *Plasmodium falciparum* erythrocyte invasion: combining function with immune evasion. *PLoS Pathog* 2014; 10: e1003943.
 12. Cowman AE, Berry D, Baum J. The cellular and molecular basis for malaria parasite invasion of the human red blood cell. *J Cell Biol* 2012; 198: 961-971.
 13. Gardner MJ, Hall N, Fung E, White O, Berriman M, Hyman RW, Carlton JM, Pain A, Nelson KE, Bowman S, Paulsen IT, James K, Eisen JA, Rutherford K, Salzberg SL, Craig A, Kyes S, Chan MS, Nene V, Shallom SJ, Suh B, Peterson J, Angiuoli S, Perlea M, Allen J, Selengut J, Haft D, Mather MW, Vaidya AB, Martin DM, Fairlamb AH, Fraunholz MJ, Roos DS, Ralph SA, McFadden GI, Cummings LM, Subramanian GM, Mungall C, Venter JC, Carucci DJ, Hoffman SL, Newbold C, Davis RW, Fraser CM, Barrell B. Genome sequence of the human malaria parasite *Plasmodium falciparum*. *Nature* 2002; 419: 498-511.
 14. Carlton JM, Adams JH, Silva JC, Bidwell SL, Lorenzi H, Caler E, Crabtree J, Angiuoli SV, Merino EF, Amedeo P, Cheng Q, Coulson RM, Crabb BS, Del Portillo HA, Essien K, Feldblyum TV, Fernandez-Becerra C, Gilson PR, Gueye AH, Guo X, Kang'a S, Kooij TW, Korsinczyk M, Meyer EV, Nene V, Paulsen I, White O, Ralph SA, Ren Q, Sargeant TJ, Salzberg SL, Stoeckert CJ, Sullivan SA, Yamamoto MM, Hoffman SL, Wortman JR, Gardner MJ, Galinski MR, Barnwell JW, Fraser-Liggett CM. Comparative genomics of the neglected human malaria parasite *Plasmodium vivax*. *Nature* 2008; 455: 757-763.
 15. Kappe SH, Noe AR, Fraser TS, Blair PL, Adams JH. A family of chimeric erythrocyte binding proteins of malaria parasites. *Proc Natl Acad Sci USA* 1998; 95: 1230-1235.
 16. Adams JH, Sim BK, Dolan SA, Fang X, Kaslow DC, Miller LH. A family of erythrocyte binding proteins of malaria parasites. *Proc Natl Acad Sci USA* 1992; 89: 7085-7089.
 17. Horuk R, Chitnis CE, Darbonne WC, Colby TJ, Rybicki A, Hadley TJ, Miller LH. A receptor for the malarial parasite *Plasmodium vivax*: the erythrocyte chemokine receptor. *Science* 1993; 261: 1182-1184.
 18. Menard D, Barnadas C, Bouchier C, Henry-Halldin C, Gray LR, Ratsimbaoa A, Thonier V, Carod JF, Domarle O, Colin Y, Bertrand O, Picot J, King CL, Grimberg BT, Mercereau-Puijalon O, Zimmerman PA. *Plasmodium vivax* clinical malaria is commonly observed in Duffy-negative Malagasy people. *Proc Natl Acad Sci USA* 2010; 107: 5967-5971.
 19. Galinski MR, Medina CC, Ingravallo P, Barnwell JW. A reticulocyte-binding protein complex of *Plasmodium vivax* merozoites. *Cell* 1992; 69: 1213-1226.
 20. Miller LH, Baruch DI, Marsh K, Doumbo OK. The pathogenic basis of malaria. *Nature* 2002; 415: 673-679.
 21. Kosaisavee V, Lek-Uthai U, Suwanarusk R, Gruner AC, Russell B, Nosten F, Renia L, Snounou G. Genetic diversity in new members of the reticulocyte binding protein family in Thai *Plasmodium vivax* isolates. *PLoS One* 2012; 7: e32105.
 22. Li J, Han ET. Dissection of the *Plasmodium vivax* reticulocyte binding-like proteins (*PvRBLs*). *Biochem Biophys Res Commun* 2012; 426: 1-6.
 23. Bozdech Z, Mok S, Hu G, Imwong M, Jaidee A, Russell B, Ginsburg H, Nosten F, Day NP, White NJ, Carlton JM, Preiser PR. The transcriptome of *Plasmodium vivax* reveals divergence and diversity of transcriptional regulation in malaria parasites. *Proc Natl Acad Sci USA* 2008; 105: 16290-16295.
 24. List C, Qi W, Maag E, Gottstein B, Muller N, Felger I. Serodiagnosis of *Echinococcus* spp. infection: explorative selection of diagnostic antigens by peptide microarray. *PLoS Negl Trop Dis* 2010; 4: e771.
 25. Noya O, Patarroyo ME, Guzman F, Alarcon de Noya B. Immunodiagnosis of parasitic diseases with synthetic peptides. *Curr Protein Pept Sci* 2003; 4: 299-308.
 26. Assis LM, Sousa JR, Pinto NF, Silva AA, Vaz AF, Andrade PP, Carvalho EM, De Melo MA. B-cell epitopes of antigenic proteins in *Leishmania infantum*: an in silico analysis. *Parasite Immunol* 2014; 36: 313-323.
 27. Singh H, Ansari HR, Raghava GP. Improved method for linear B-cell epitope prediction using antigen's primary sequence. *PLoS One* 2013; 8: e62216.
 28. Saha S, Raghava GPS. BcePred: Prediction of continuous B-cell epitopes in antigenic sequences using physico-chemical proper-

- ties. Artificial Immune Systems, Proceedings 2004; 3239: 197-204.
29. Saha S, Raghava GP. Prediction of continuous B-cell epitopes in an antigen using recurrent neural network. *Proteins* 2006; 65: 40-48.
 30. Larsen JE, Lund O, Nielsen M. Improved method for predicting linear B-cell epitopes. *Immunome Res* 2006; 2: 2.
 31. Yang X, Yu X. An introduction to epitope prediction methods and software. *Rev Med Virol* 2009; 19: 77-96.
 32. Mahdavi M, Mohabatkar H, Keyhanfar M, Dehkordi AJ, Rabbani M. Linear and conformational B cell epitope prediction of the HER 2 ECD-subdomain III by in silico methods. *Asian Pac J Cancer Prev* 2012; 13: 3053-3059.
 33. Bouillon A, Giganti D, Benedet C, Gorgette O, Petres S, Crublet E, Girard-Blanc C, Witkowski B, Menard D, Nilges M, Mercereau-Puijalon O, Stoven V, Barale JC. In Silico screening on the three-dimensional model of the *Plasmodium vivax* SUB1 protease leads to the validation of a novel anti-parasite compound. *J Biol Chem* 2013; 288: 18561-18573.
 34. Restrepo-Montoya D, Becerra D, Carvajal-Patino JG, Mongui A, Nino LF, Patarroyo ME, Patarroyo MA. Identification of *Plasmodium vivax* proteins with potential role in invasion using sequence redundancy reduction and profile hidden Markov models. *PLoS One* 2011; 6: e25189.
 35. Cheng Y, Wang Y, Ito D, Kong DH, Ha KS, Chen JH, Lu F, Li J, Wang B, Takashima E, Sattabongkot J, Tsuboi T, Han ET. The *Plasmodium vivax* merozoite surface protein 1 paralog is a novel erythrocyte-binding ligand of *P. vivax*. *Infect Immun* 2013; 81: 1585-1595.
 36. Cespedes N, Habel C, Lopez-Perez M, Castellanos A, Kajava AV, Servis C, Felger I, Moret R, Arevalo-Herrera M, Corradin G, Herrera S. *Plasmodium vivax* antigen discovery based on alpha-helical coiled coil protein motif. *PLoS One* 2014; 9: e100440.
 37. Crowther GJ, Shanmugam D, Carmona SJ, Doyle MA, Hertz-Fowler C, Berriman M, Nwaka S, Ralph SA, Roos DS, Van Voorhis WC, Aguero F. Identification of attractive drug targets in neglected-disease pathogens using an in silico approach. *PLoS Negl Trop Dis* 2010; 4: e804.
 38. Kulangara C, Kajava AV, Corradin G, Felger I. Sequence conservation in *Plasmodium falciparum* alpha-helical coiled coil domains proposed for vaccine development. *PLoS One* 2009; 4: e5419.
 39. Olugbile S, Villard V, Bertholet S, Jafarshad A, Kulangara C, Roussillon C, Frank G, Agak GW, Felger I, Nebie I, Konate K, Kajava AV, Schuck P, Druilhe P, Spertini F, Corradin G. Malaria vaccine candidate: design of a multivalent subunit alpha-helical coiled coil poly-epitope. *Vaccine* 2011; 29: 7090-7099.
 40. Neafsey DE, Galinsky K, Jiang RH, Young L, Sykes SM, Saif S, Gujja S, Goldberg JM, Young S, Zeng Q, Chapman SB, Dash AP, Anvikar AR, Sutton PL, Birren BW, Escalante AA, Barnwell JW, Carlton JM. The malaria parasite *Plasmodium vivax* exhibits greater genetic diversity than *Plasmodium falciparum*. *Nat Genet* 2012; 44: 1046-1050.
 41. Bowman S, Lawson D, Basham D, Brown D, Chillingworth T, Churcher CM, Craig A, Davies RM, Devlin K, Feltwell T, Gentles S, Gwilliam R, Hamlin N, Harris D, Holroyd S, Hornsby T, Horrocks P, Jagels K, Jassal B, Kyes S, McLean J, Moule S, Mungall K, Murphy L, Oliver K, Quail MA, Rajandream MA, Rutter S, Skelton J, Squares R, Squares S, Sulston JE, Whitehead S, Woodward JR, Newbold C, Barrell BG. The complete nucleotide sequence of chromosome 3 of *Plasmodium falciparum*. *Nature* 1999; 400: 532-538.
 42. Hall N, Pain A, Berriman M, Churcher C, Harris B, Harris D, Mungall K, Bowman S, Atkin R, Baker S, Barron A, Brooks K, Buckee CO, Burrows C, Cherevach I, Chillingworth C, Chillingworth T, Christodoulou Z, Clark L, Clark R, Corton C, Cronin A, Davies R, Davis P, Dear P, Dearden F, Doggett J, Feltwell T, Goble A, Goodhead I, Gwilliam R, Hamlin N, Hance Z, Harper D, Hauser H, Hornsby T, Holroyd S, Horrocks P, Humphray S, Jagels K, James KD, Johnson D, Kerhornou A, Knights A, Konfortov B, Kyes S, Larke N, Lawson D, Lennard N, Line A, Maddison M, McLean J, Mooney P, Moule S, Murphy L, Oliver K, Ormond D, Price C, Quail MA, Rabbinowitsch E, Rajandream MA, Rutter S, Rutherford KM, Sanders M, Simmonds M, Seeger K, Sharp S, Smith R, Squares R, Squares S, Stevens K, Taylor K, Tivey A, Unwin L, Whitehead S, Woodward J, Sulston JE, Craig A, Newbold C, Barrell BG. Sequence of *Plasmodium falciparum* chromosomes 1, 3-9 and 13. *Nature* 2002; 419: 527-531.
 43. Villard V, Agak GW, Frank G, Jafarshad A, Servis C, Nebie I, Siriima SB, Felger I, Arevalo-Herrera M, Herrera S, Heitz F, Backer V, Druilhe P, Kajava AV, Corradin G. Rapid identification of malaria vaccine candidates based on alpha-helical coiled coil protein motif. *PLoS One* 2007; 2: e645.
 44. Tran TM, Oliveira-Ferreira J, Moreno A, Santos F, Yazdani SS, Chitnis CE, Altman JD, Meyer EV, Barnwell JW, Galinski MR. Comparison of IgG reactivities to *Plasmodium vivax* merozoite invasion antigens in a Brazilian Amazon population. *Am J Trop Med Hyg* 2005; 73: 244-255.
 45. Rayner JC, Tran TM, Corredor V, Huber CS, Barnwell JW, Galinski MR. Dramatic difference in diversity between *Plasmodium falciparum* and *Plasmodium vivax* reticulocyte binding-like genes. *Am J Trop Med Hyg* 2005; 72: 666-674.
 46. Prajapati SK, Kumari P, Singh OP. Molecular analysis of reticulocyte binding protein-2 gene in *Plasmodium vivax* isolates from India. *BMC Microbiol* 2012; 12: 243.